Preprint typeset using LaTeX style emulateapj v. 11/10/09

A NEW CLASSIFICATION METHOD FOR GAMMA-RAY BURSTS

Hou-Jun Lü[1], En-Wei Liang[1,2], Bin-Bin Zhang[2], and Bing Zhang[2]

ABSTRACT

Recent *Swift* observations suggest that the traditional long vs. short GRB classification scheme does not always associate GRBs to the two physically motivated model types, i.e. Type II (massive star origin) vs. Type I (compact star origin). We propose a new phenomenological classification method of GRBs by introducing a new parameter $\varepsilon = E_{\gamma,\rm iso,52}/E^{5/3}_{p,z,2}$, where $E_{\gamma,\rm iso}$ is the isotropic gamma-ray energy (in units of 10^{52}erg), and $E_{\rm p,z}$ is the cosmic rest frame spectral peak energy (in units of 100 keV). For those short GRBs with "extended emission", both quantities are defined for the short/hard spike only. With the current complete sample of GRBs with redshift and E_p measurements, the ε parameter shows a clear bimodal distribution with a separation at $\varepsilon \sim 0.03$. The high-ε region encloses the typical long GRBs with high-luminosity, some high-z "rest-frame-short" GRBs (such as GRB 090423 and GRB 080913), as well as some high-z short GRBs (such as GRB 090426). All these GRBs have been claimed to be of the Type II origin based on other observational properties in the literature. All the GRBs that are argued to be of the Type I origin are found to be clustered in the low-ε region. They can be separated from some nearby low-luminosity long GRBs (in 3σ) by an additional T_{90} criterion, i.e. $T_{90,z} \lesssim 5$ s in the *Swift*/BAT band. We suggest that this new classification scheme can better match the physically-motivated Type II/I classification scheme.

Subject headings: gamma-ray bursts: general — methods: statistical

1. INTRODUCTION

Phenomenologically, gamma-ray bursts (GRBs) are classified as long *vs.* short with a division line at the observed duration $T_{90} \sim 2$ s (Kouveliotou et al. 1993). Robust associations of the underlying supernovae (SNe) with some long GRBs (Galama et al. 1998; Stanek et al. 2003; Hjorth et al. 2003; Malesani et al. 2004; Modjaz et al. 2006; Pian et al. 2006) and the fact that long GRB host galaxies are typically irregular galaxies with intense star formation (Fruchter et al. 2006) suggest that they are likely related to the deaths of massive stars, and the "collapsar" model has been widely recognized as the standard scenario for long GRBs (Woosley 1993; Paczyński 1998; Woosley & Bloom 2006). Observational breakthroughs led by the *Swift* mission (Gehrels et al. 2004) suggest that at least some short GRBs are associated with nearby host galaxies with little star formation (Tanvir et al. 2005), and that they are not associated with an underlying SN (Gehrels et al. 2005; Villasenor et al. 2005; Fox et al. 2005; Hjorth et al. 2005; Berger et al. 2005), favoring the idea that they are produced by mergers of two compact stellar objects, such as NS-NS and NS-BH mergers (Eichler et al. 1989; Narayan et al. 1992; Nakar 2007).

However, several lines of observational evidence in the *Swift* era suggest that duration is not necessarily a reliable indicator of the physical nature of a GRB. (1) The non-detection of a SN signature associated with the nearby long GRBs 060614 and 060505 (Gehrels et al. 2006; Gal-Yam et al. 2006; Fynbo et al. 2006; Della Valle et al. 2006) disfavors the conventional collapsar scenario of long GRBs (Woosley & Bloom 2006). Some observational properties of the ~ 100 s long GRB 060614 are very similar to those of some short GRBs (Gehrels et al. 2006; Zhang et al. 2007), making it likely associated with the physical category that most short GRBs belong to. (2) Significant soft "extended" gamma-ray emission and late X-ray flares are observed in a handful of "short" GRBs (Barthelmy et al. 2005; Norris & Bonnell 2006; Perley et al. 2009), suggesting that they are not necessarily short. A new physically motivated classification scheme, i.e., Type II (massive star origin) vs. Type I (compact star origin) was proposed (Zhang 2006; Zhang et al. 2007). Kann et al (2010, 2008) systematically studied the optical afterglow emission properties of Type II and Type I GRBs, and suggested that these properties carry important information about the nature of GRB progenitors. A full definition of Type I/II GRBs as well as the multiple observational criteria are presented in Zhang et al. (2009). (3) Two high-redshift gamma-ray bursts, GRB 080913 at $z = 6.7$ (Greiner et al. 2009; Perez-Ramirez et al. 2010) and GRB 090423 at $z = 8.2$ (Tanvir et al. 2009; Salvaterra et al. 2009), appear as intrinsically short GRBs. Their observed durations are (8 ± 1)s and ~ 10.3s in the *Swift/BAT* band, respectively. Corrected redshift, the durations of two high-z GRBs are shorter than 2 seconds in the rest frame. The physical origin of these high-z GRBs have been subject to debate (Greiner et al. 2009; Perez-Ramirez er al. 2010; Tanvir et al. 2009; Salvaterra et al.2009). Although compact star mergers may occur at such a high redshift (Belczynski et al. 2010), various observational properties of these two GRBs point towards the massive star origin (Zhang et al. 2009; Lin et al. 2009; Belczynki et al. 2010). (4) A more striking case is GRB 090426, whose observed BAT band T_{90} is only 1.2 ± 0.3s, and the rest frame duration is only ~ 0.33 s at $z = 2.609$ (Levesque et al. 2009). It greatly exceeds the previous short GRB redshift record, i.e. $z = 0.923$ for GRB 070714B (Graham et

[1] Department of Physics, Guangxi University, Nanning 530004, China; lew@gxu.edu.cn
[2] Department of Physics and Astronomy, University of Nevada, Las Vegas, NV 89154. zhang@physics.unlv.edu

al. 2009). Phenomenologically, this is an unambiguous short-duration GRB, but the available afterglow and host galaxy properties point towards a different picture: it has a blue, very luminous, star-forming putative host galaxy with a small angular offset of the afterglow location from the center, and a similar medium density as typical Type II GRBs. All these suggest that the burst is more closely related to the core collapse of a massive star (Levesque et al. 2009; Antonelli et al. 2009; Xin et al. 2010). (5) Monte Carlo simulations suggest that the compact star merger model cannot interpret both the *Swift* z-known short GRB sample and the BATSE short GRB sample. Instead one may need a mix of GRBs from compact star mergers and from massive star core collapses to account for the observed short GRB population (Virgili et al. 2009; Cui et al. 2010).

In summary, the traditional long *vs.* short GRB scheme no longer always correspondingly match the two distinct physical origins, i.e., collapse of massive stars (Type II GRBs) *vs.* mergers of compact stars (Type I GRBs) (Zhang 2006; Zhang et al. 2007, 2009; Bloom et al. 2008). Zhang et al (2009) proposed a procedure (a flow chart, see their Fig.8) invoking a full set of observational characteristics, including supernova(SN)-GRB association, specific star-forming rate (SFR) of the host galaxy, burst location offset, burst duration, hardness, spectral lag, statistical correlations, energetics, and afterglow properties, to judge the physical category of a GRB. On the other hand, for most GRBs one may not immediately retrieve all the information needed for such a classification. It would be interesting to search for additional phenomenological classification schemes to see whether there exist other quantities, especially those invoking prompt GRB emission properties only, that can give a good indication of the physical nature of a GRB. This motivates us to explore a new phenomenological classification method. Besides the burst duration, we think both the burst energy and the spectral properties in the burst rest frame would carry important information about the nature of the burst. In this paper, we propose a new discriminator based on the isotropic burst energy and rest frame peak energy ($E_{\rm p}$) of the νf_ν spectrum of the prompt gamma-rays. We will show that this classification method is more closely connected to the Type II/I physical classification scheme.

2. SAMPLE

In order to develop our classification method, we use a sample of all GRBs with both redshift and spectral parameters known up to Mar, 2010. Our sample includes 137 GRBs. They are detected by *BeppoSAX*, *HETE-2*, *Swift*, *Suzaku*, and *Fermi*. Most of them are taken from Amati et al. (2008, 2009), Kann et al. (2010), Krimm et al. (2009), Zhang et al. (2009) and references therein. Their isotropic gamma-ray energy ($E_{\gamma,iso}$) is calculated in the GRB rest-frame $1-10^4$ kev band with the spectral parameters in order to avoid instrument selection effect. The soft XRF 080109 (Soderberg et al. 2008), whose emission is in the XRT band (0.3-10kev) instead of BAT band, is also included in our sample. The XRT and UVOT observations place a limit of its E_p in the range 0.037 kev $< E_{peak} <$ 0.3 kev. We adopt $E_{peak} \approx 0.12^{+0.23}_{-0.089}$ kev (Li 2008). Eight bursts in our sample (GRBs 050709, 050724, 051210, 060614, 061006, 061210, 070714B, and 071227) are the so-called short GRBs with "extended emission" discussed in literature. For these GRBs, both parameters ($E_{\gamma,iso}$ and $E_{p,z}$) are derived for the initial hard spike only (extended emission excluded)[3]. We tabulate only those GRBs with $T_{90,z} = T_{90}/(1+z) < 2$ s (Twenty-nine GRBs) in our sample in Table 1.

3. A NEW GRB CLASSIFICATION PARAMETER

Firstly, we show the distribution of $T_{90,z}$ in Fig. 1(a). Similar to that shown in Lin et al. (2009), $T_{90,z}$ for the current GRB sample with redshift measurements has a tentative bimodal distribution, with peaks at $\log T_{90,z} = -0.5$ and 1.25, respectively. Due to the overlap between the two classes (long vs. short), those GRBs having $T_{90,z} = 1 \sim 5$ seconds cannot be unambiguously categorized into either group[4]. We test the bimodality with the KMM algorithm presented by Ashman et al. (1994), and obtain a chance probability $p \sim 10^{-2}$. The correct allocation rate for short GRBs estimated with the KMM algorithm is 73.3%.

We develop our classification method by defining a parameter,

$$\varepsilon(\kappa) \equiv E_{\gamma,\rm iso,52}/E^{\kappa}_{\rm p,z,2}, \quad (1)$$

where $E_{\gamma,\rm iso,52} = E_{\gamma,\rm iso}/10^{52}$ ergs and $E_{\rm p,z} = E_p(1+z)/10^2$ keV. Note that ε does not depend on any spectrum - energy correlation or theoretical assumption. We explore various κ values, and found that given a same observed GRB (known fluence and E_p) the implicit z-dependence of $\varepsilon(\kappa) \propto D_L^2(z)/(1+z)^{1+\kappa}$ essentially vanishes at $z > 2$, if $\kappa = 5/3$ (see Fig. 2 for a comparison of the z-dependence of ε for different κ). We therefore define

$$\varepsilon \equiv E_{\gamma,\rm iso,52}/E^{5/3}_{\rm p,z,2}, \quad (2)$$

which removes the redshift dependence for high-z GRBs. This parameter may be more suitable for the classification of high-z GRBs, such as GRBs 090423 and 080913.

We calculate ε for the bursts in our sample and show the $\log\varepsilon$ distribution in Fig.1 (b). A clear bimodal feature is found, with a division line at ~ 0.03 (high-ε vs. low-ε). The high-ε portion follows a log normal distribution with $\varepsilon = 0.80 \pm 0.11$ (1σ). For the low-ε it is 0.003 ± 0.002. We test the bimodality of the ε distribution with the KMM algorithm and obtain a chance

[3] We note that T_{90} depends on the detector's sensitivity and energy band. In our analysis, we define T_{90} using the BAT energy band and sensitivity. In the *Swift* era, it is found that some "short" GRBs (as observed in the BATSE band) have extended emission. It is the convention of the *Swift* team and the community to define a "short" GRB based on the duration of the short spike only, with the extended emission excluded. Observationally, the spectrum of the short spike is much harder than that of the extended emission, the latter shares many properties with X-ray flares. For a same burst, the "extended emission" depends on redshift, since it may be buried within the background if the redshift is high enough. We therefore only use the information of the short/hard spike to perform our classification.

[4] It was proposed that those GRBs having $T_{90,z} = 1 \sim 5$ seconds may be an intermediate population based on the excess of the GRBs over the bimodal distribution of $T_{90,z}$. Although these GRBs are less energetic and have dimmer afterglows than typical long GRBs, they share many similar properties of typical GRBs, such as spectral lag and spectrum-energy correlations. They may be a sub-group of the long GRBs (de Ugarte Postigo 2010).

probability $p < 10^{-4}$. The overall correct allocation rate of GRBs in the two categories (high-ε vs. low-ε) is as high as 99.8%, indicating that ε is a new parameter for GRB classification.

It is generally believed that GRBs originate either from core collapses of massive stars (Type II) or mergers of compact stars (Type I). One may ask whether this phenomenal classification matches the physical scheme of the Type I and Type II. The origins of most GRBs in our sample have been extensively discussed in literature (Zhang et al. 2009; Kann et al. 2010, 2008). We therefore examine how the members in our two new categories (high-ε vs. low-ε) are associated with the two physical model types. To define the physical category of the GRBs, we apply the flow chart of Zhang et al. (2009, their Fig.8). We denote all "Type II" or "Type II candidates" as "Type II", and "Type I" or "Type I candidates" as "Type I" (which include the Type I Gold sample and most other short/hard GRBs in Zhang et al. 2009). We note that these definitions are fully consistent with those adopted in Kann et al. (2010, 2008). Fig. 1 displays all the GRBs in our sample in the $\varepsilon - T_{90,z}$ plane. Different symbols are used to mark different groups. For example, triangles denote the GRBs that are believed to be of the Type II origin, among which the black triangles denote the traditional long GRBs, and the blue triangles denote the GRBs those with $T_{90,z}$'s shorter than 2 s. The red circles denote those GRBs that are believed to have the Type I origin. Six green stars denote nearby low luminosity GRBs with supernova associations. It is remarkable to see that the ε classification clearly separates Type II GRBs from Type I GRBs.

In order to quantitatively assess the clustering feature among different types of GRBs, we derive the GRB distribution probability $p(\log\varepsilon, \log T_{90,z})$ from the ratio between the number of GRBs in the grid $\log\varepsilon + d\log\varepsilon, \log T_{90,z} + d\log T_{90,z}$ and the total number of GRBs in our sample. Since the distribution of ε is concerned in our analysis, we take the error of $\log\varepsilon$ into account in our calculation of p. For a given GRB with $\log\varepsilon \pm \delta\log\varepsilon$, we assume that the probability distribution of this GRB is a normalized log-normal distribution centering at $\log\varepsilon$ with a width of $\delta\log\varepsilon$. The probability (p_i) of the GRB in a given rage $[\log\varepsilon - d\log\varepsilon/2, \log\varepsilon + d\log\varepsilon/2]$ is calculated by integrating the probability distribution function in the range. The probability $p(\log\varepsilon, \log T_{90,z})$ is then obtained by summing up p_i over the GRBs in our sample. We take $d\log T_{90,z} = 0.35$ and $d\log\varepsilon = 0.60$ in our calculation. The contours of the probability distribution are shown in Fig. 1(c). One can clearly identify two clustering regions [with $p(\log\varepsilon, \log T_{90,z}) > 0.1$] centered in the high-$\varepsilon$ regime and the low-ε, low-$T_{90,z}$ regime. At the 3σ level, the high-ε group includes typical long GRBs with high-luminosity, some intrinsic short duration GRBs (including the high-z GRB 090423 and GRB 080913), as well as some high-z short GRBs (e.g. GRB 090426). In contrast, the low-ε group contains the extensively discussed Type I GRBs, including those with and without extended emission. Based on the probability contours, a low-ε GRB with $T_{90,z} \lesssim 5$ s in the *Swift*/BAT band would be identified as a Type I GRB at the 3σ confidence level. GRBs 060614 and 060505 are marginally included in the $p(\log\varepsilon, \log T_{90,z}) > 0.003$ region (the light grey region in Fig. 1c) of the Type I GRBs. Nearby low luminosity long GRBs (LL-GRBs), e.g. GRBs 980425, 031203, 050826, and 060218 (green stars in Fig. 1c) are out of the 3 σ contours of the Type I and Type II GRBs. This may hint a distinct GRB population as suggested by Liang et al. (2007; see also Soderberg et al. 2004; Cobb et al. 2006).

4. CONCLUSIONS AND DISCUSSION

By introducing a new parameter ε, we have proposed a new phenomenological classification method for GRBs. We demonstrated that GRBs with known redshifts are cozily classified into two classes with a separation $\varepsilon = 0.03$. Due to the clear bimodal distribution of ε with little overlap, the overall correct allocation rate of a GRB to a particular category (high-ε vs. low-ε) is as high as $> 99.8\%$, which is much better than the traditional duration classification method. More importantly, this classification scheme is more closely related to the two physically motivated model classes - Type II vs. I. In particular, the high-ε category is a good representation of the Type II GRBs, while the low-ε category, with an additional duration criterion $T_{90,z} \lesssim 5$ s, is a good representation of the Type I GRBs. We suggest that the ε parameter can be evaluated for future GRBs with z measurements, and the ε-based classification may be performed regularly to infer the physical origin of a GRB.

The well-separated bimodal distribution of $\log\varepsilon$ depends on our selection of κ in Eq. (1). As shown in Fig. 2, ε is insensitive to z at $z > 2$ for a given burst by taking $\kappa = 5/3$, but it is not at low redshift. One may suspect that if the bimodal distribution is due to the redshift effect. To examine this issue, we re-plot the Figure 1 by separating GRBs into the $z > 2$ and the $z < 2$ samples (Figure 3, left and middle panels, respectively). We also show the GRB distributions in the $\log(1+z) - \log(\varepsilon)$ plane for all the bursts in our sample in Figure 3. It is found that the the clustering feature of $\log\varepsilon$ is not caused by the redshift selection effect. Therefore, ε is a GRB discriminator for both GRBs at $z < 2$ and $z > 2$.

Another concern about our classification method may be sample uniformity. The GRBs in our sample were detected with different instruments with different instrumental threshold. However, our classification method is based on the global energy and spectral information. Different from the burst duration, a well-measured E_p essentially does not depend on the detector. So is $E_{\gamma,\rm iso}$. The E_p values of the GRBs in our sample, which expand almost four orders of magnitude, are well within the energy band of previous and current GRB missions, so they are well measured. The $E_{\rm iso}$ values expand almost eight orders of magnitude. Therefore, our sample could be regarded as a complete sample with known E_p and $E_{\rm iso}$ for current missions.

We should note that our classification scheme is particularly helpful to diagnose the physical origin of GRBs with a rest-frame short duration (e.g. $T_{90,z} < 2$ s, Table 1). For example, it convincingly classifies GRBs 090423, 080913 and 090426 into the high-ε, and therefore, the Type II category, which is otherwise difficult with the duration criterion[5]. The distinction of the $T_{90,z} < 2s$ bursts

[5] As shown in Figure 2, a GRB with the same observed fluence and E_p at higher redshift may have a higher ε. However, the bimodal distribution may not be due to the redshift effect (see

with different ε values is also evident from their X-ray afterglow properties. Kann et al. (2008) compared the optical afterglows Type I GRBs with Type II GRBs, and found that those of Type I GRBs have a lower average luminosity and show a larger intrinsic spread of luminosities. In Figure 4, we compare the XRT lightcurves and the 12-hour X-ray luminosities between the two types of $T_{90,z} < 5s$ s GRBs. The low-ε $T_{90,z} < 2s$ s GRBs (Type I, red) are systematically fainter than the high-ε ones (Type II, blue)[6], whose properties are rather similar to other high-ε long GRBs (black).

Physically it is not obvious why the parameter ε (corresponding to $\kappa = 5/3$) gives a cozy classification scheme. We have tried other κ values in Eq.(1), but the classifications defined by other $\varepsilon(\kappa)$ are not as clean as the one defined by Eq.(2). As shown in Figure 2, an apparent advantage of $\kappa = 5/3$ is to diminish the z-dependence at high-z for a given observed GRB.

One can also discuss the connection between the lognormal distribution of ε in the high-ε regime and some empirical relations of Type II GRBs. With the Amati-relation $E_{p,z} \propto E_{\gamma,\rm iso}^{0.54}$ (Amati et al. 2009), we find that $\varepsilon \propto E_{\rm p,z}^{0.185}$, insensitive to $E_{\rm p,z}$. Liang & Zhang (2005) discovered an empirical relation among $E_{\gamma,\rm iso}$, $E_{\rm p,z}$, and $t_{\rm b,z}$, namely, $E_{\gamma,\rm iso} \propto E_{\rm p,z}^{1.94\pm0.17} t_{\rm b,z}^{-1.24\pm0.23}$, where $t_{\rm b,z}$ is the rest-frame break time of the optical afterglow lightcurve. This gives $\varepsilon \propto E_{\rm p,z}^{0.27\pm0.17} t_{\rm b,z}^{-1.24\pm0.23}$, which is sensitive to $t_{\rm b,z}$. A clustering in ε therefore corresponds to a clustering in $t_{\rm b,z}$. Interpreting the $t_{\rm b,z}$ as the jet break time, the Liang-Zhang relation may be translated into the Ghirlanda-relation, $E_{\gamma,\rm iso,52}(1 - cos\theta_j) \simeq A E_{\rm p,z,2}^{\sim 1.7}$, where $A \sim 0.01 - 0.03$ (Ghirlanda et al. 2004; Dai et al. 2004). Given $\varepsilon \equiv E_{\gamma,\rm iso,52}/E_{\rm p,z,2}^{1.7}$, we can get $\varepsilon \approx A(1-\cos\theta_j)^{-1}$, where θ_j is the jet opening angle. The lognormal ε distribution ($\varepsilon = 0.80 \pm 0.11$, at 1σ) therefore corresponds to a lognormal jet opening angle distribution for Type II GRBs, i.e., $\theta_j \sim 0.16 \pm 0.03$ rad (assuming $A \sim 0.01$). We note that the jet opening angle derived by Ghirlanda et al. (2004) indeed clusters in a small range. Since the Ghirlanda-relation is very difficult to understand physically, we suspect that it may be related the fact that ε is quasi-universal for Type II GRBs. Future data with very early or very late optical break times may test whether the Ghirlanda/Liang-Zhang relations or the fact of a quasi-universal ε are more fundamental.

We acknowledge the use of the public data from the *Swift* and *Fermi* data and GCN circulars archive. We thank helpful comments from the referee. This work is supported by the National Natural Science Foundation of China (Grants 11025313, 10873002, 11078008), the National Basic Research Program ("973" Program) of China (Grant 2009CB824800), Guangxi SHI-BAI-QIAN project (Grant 2007201), Guangxi Science Foundation (2010GXNSFC013011), the program for 100 Young and Middle-aged Disciplinary Leaders in Guangxi Higher Education Institutions, and the research foundation of Guangxi University. It is also partially supported by NASA NNX09AT66G, NNX10AD48G, and NSF AST-0908362.

Figure 3).

[6] We cannot exclude the possibility that this is a selection effect, since high-z Type I GRBs may have fainter X-ray afterglows and therefore may not be detected.

REFERENCES

Abdo, A. A., et al. 2009, Nature, 462, 331
Amati, L., Guidorzi, C., Frontera, F., et al. 2008, MNRAS, 391, 577
Amati, L., Frontera, F., & Guidorzi, C. 2009, A&A, 508, 173
Antonelli, L. A., et al. 2009, A&A, 507, L45
Ashman, K. M., Bird, C. M., & Zepf, S. E. 1994, AJ, 108, 2348
Barthelmy, S. D., et al. 2005, Nature, 438, 994
Belczynski, K., Holz, D. E., Fryer, C. L., et al. 2010, ApJ, 708, 117
Berger, E., Price, P.A., Cenko, S.B., et al. 2005, Nature, 438, 988
Bloom, J. S., Butler, N. R., & Perley, D. A. 2008, AIPC, 1000, 11
Butler, N. R., Kocevski, D., Bloom, J. S., et al. 2007, ApJ, 671, 656
Cenko, S. B., et al. 2010, GCN, 10389, 1
Cobb, B. E., Bailyn, C. D., van Dokkum, P. G., & Natarajan, P. 2006, ApJ, 645, L113
Cui, X.-H., Aoi, J., Nagataki, S., & Xu, R.-X. 2010, arXiv:1004.2302
Dai, Z. G., Liang, E. W., & Xu, D. 2004, ApJ, 612, L101
de Ugarte Postigo, A., et al. 2010, arXiv:1006.4469
Della Valle, M., et al. 2006, Nature, 444, 1050
Eichler, D., Livio, M., Piran, T., & Schramm, D. N. 1989, Nature, 340, 126
Fox, D.B., Frail, D.A., Price, P.A., et al. 2005, Nature, 437, 845
Fruchter, A.S., Levan, A.J., Strolger, L., et al. 2006, Nature, 441, 463
Fynbo, J.P.U., Watson, D., Thöne, C.C., et al. 2006, Nature, 444, 1047
Galama, T. J., et al. 1998, Nature, 395, 670
Gal-Yam, A., Fox, D.B., Price, P.A., et al. 2006, Nature, 444, 1053
Gehrels, N., et al. 2004, ApJ, 611, 1005
Gehrels, N., Sarazin, C.L., O'Brien, P.T., et al. 2005, Nature, 437, 851
Gehrels, N., Norris, J.P., Barthelmy, S.D., et al. 2006, Nature, 444, 1044
Ghirlanda, G., Ghisellini, G., & Lazzati, D. 2004, ApJ, 616, 331
Graham, J. F., et al. 2009, ApJ, 698, 1620
Greiner, J., Krühler, T., McBreen, S., et al. 2009, ApJ, 693, 1610
Hjorth, J., Sollerman, J., Møller, P., et al. 2003, Nature, 423, 847
Hjorth, J., et al. 2005, Nature, 437, 859
Kann, D. A., et al. 2008, arXiv:0804.1959
Kann, D. A., et al. 2010, ApJ, 720, 1513
Kouveliotou, C., Meegan, C. A., Fishman, G. J., et al 1993, ApJ, 413, L101
Krimm, H. A., et al. 2009, ApJ, 704, 1405
Li, L.-X. 2008, MNRAS, 388, 603
Levesque, E. M., et al. 2009, MNRAS, 1657
Liang, E.-W., & Zhang, B. 2005, ApJ, 633, 611
Liang, E. -W, Zhang, B., Virgili, F., & Dai, Z. G. 2007, ApJ, 662, 1111
Liang, E.-W., Lü, H.-J., Hou, S.-J., et al. 2009, ApJ, 707, 328
Lin, L., Liang, E. -W., & Zhang, S. N. 2010, Science in China G: Physics and Astronomy, 53, 64
Malesani, D., et al. 2004, ApJ, 609, L5
Modjaz, M., et al. 2006, ApJ, 645, L21
Nakar, E. 2007, Phys. Rep., 442, 166
Narayan, R., Paczynski, B., & Piran, T. 1992, ApJ, 395, L83
Norris, J. P., & Bonnell, J. T. 2006, ApJ, 643, 266
Paczynski, B. 1998, ApJ, 494, L45
Pérez-Ramírez, D., et al. 2010, A&A, 510, A105
Perley, D.A., Metzger, B.D., Granot, J., et al. 2009, ApJ, 696, 1871
Pian, E., Mazzali, P.A., Masetti, N., et al. 2006, Nature, 442, 1011
Piranomonte, S., et al. 2006, GCN, 5626, 1
Sakamoto, T., et al. 2008, GCN, 7761, 1
Salvaterra, R., et al. 2009, Nature, 461, 1258

TABLE 1
THE SAMPLE OF 29 GRBS FOR $T_{90,z} < 2$ S IN THE REST FRAME.

GRB name	z redshift	$T_{90,z}$ (s)	EE (s)	$E_{\rm p}$ (KeV)	$E_{\gamma,\rm iso}$ (10^{52} erg)	log ε	Type	Afterglow X/O(IR)	Refs.
050406	2.44	1.57	n/a	25^{+25}_{-19}	$0.14^{+0.13}_{-0.03}$	$-0.74^{+0.73}_{-0.55}$	high-ε (II)	Y / Y	(1)
050416A	0.6535	1.51	n/a	$15^{+2.5}_{-2.5}$	$0.1^{+0.01}_{-0.01}$	$0.00^{+0.12}_{-0.12}$	high-ε (II)	Y / Y	(2)
050509B	0.2248	0.06	n/a	82^{+611}_{-80}	$2.4^{+4.4}_{-4} \times 10^{-4}$	$-3.62^{+1.21}_{-0.51}$	low-ε (I)	N / N	(1,3)
050709	0.1606	0.09	130±7	83^{+18}_{-12}	$2.7^{+1.1}_{-1.1} \times 10^{-3}$	$-2.54^{+0.16}_{-0.11}$	low-ε (I)	N / N	(1,3)
050724*	0.2576	2.39	154±1	110^{+400}_{-45}	$9^{+19}_{-2} \times 10^{-3}$	$-2.28^{+0.74}_{-0.30}$	low-ε (I)	Y / N	(1,3)
050813	∼0.72	∼0.26	n/a	210^{+710}_{-130}	$1.5^{+2.5}_{-0.8} \times 10^{-2}$	$-2.75^{+1.12}_{-0.45}$	low-ε (I)	N / N	(1,3)
050922C	2.198	1.41	n/a	130^{+35}_{-35}	$5.3^{+1.7}_{-1.7}$	$-0.31^{+0.19}_{-0.19}$	high-ε (II)	Y / Y	(2)
051221A	0.5464	0.91	n/a	402^{+72}_{-93}	$0.28^{+0.21}_{-0.1}$	$-1.88^{+0.13}_{-0.17}$	low-ε (I)	Y / N	(3)
060206	4.048	1.51	n/a	78^{+9}_{-9}	$4.3^{+0.9}_{-0.9}$	$-0.36^{+0.10}_{-0.10}$	high-ε (II)	Y / Y	(2)
060502B	0.287	0.10	n/a	340^{+720}_{-190}	$3^{+5}_{-2} \times 10^{-3}$	$-3.59^{+1.14}_{-0.41}$	low-ε (I)	N / N	(1,3)
060614*	0.1254	∼4.44	106±3	302^{+214}_{-85}	$0.24^{+0.04}_{-0.04}$	$-1.68^{+0.51}_{-0.21}$	low-ε (I)	Y / Y	(2,3)
060801	1.131	0.23	n/a	620^{+1070}_{-340}	$0.17^{+0.021}_{-0.021}$	$-2.64^{+1.01}_{-0.40}$	low-ε (I)	Y / N	(1,3)
060926	3.208	1.90	n/a	19^{+8}_{-18}	$0.42^{+0.59}_{-0.04}$	$0.16^{+0.31}_{-0.69}$	high-ε (II)	Y / N	(1,4)
061006	0.4377	∼0.35	120	640^{+144}_{-227}	$0.22^{+0.12}_{-0.12}$	$-2.26^{+0.16}_{-0.26}$	low-ε (I)	Y / N	(1,3)
061201	0.111	0.54	n/a	873^{+458}_{-284}	$0.018^{+0.002}_{-0.015}$	$-3.39^{+0.38}_{-0.24}$	low-ε (I)	Y / N	(1,3)
061210	0.4095	0.57	85±5	540^{+760}_{-310}	$0.09^{+0.16}_{-0.05}$	$-2.51^{+0.82}_{-0.42}$	low-ε (I)	N / N	(1,3)
061217	0.827	0.22	n/a	400^{+810}_{-210}	$0.03^{+0.04}_{-0.02}$	$-2.96^{+0.47}_{-0.38}$	low-ε (I)	N / N	(1,3)
070429B	0.9023	0.25	n/a	120^{+746}_{-66}	$0.03^{+0.01}_{-0.01}$	$-2.13^{+0.75}_{-0.40}$	low-ε (I)	N / N	(1,3)
070506	2.31	1.30	n/a	71^{+95}_{-25}	$0.26^{+0.17}_{-0.05}$	$-1.20^{+0.67}_{-0.26}$	high-ε (II)	Y / N	(1,5)
070714B	0.9225	∼1.56	∼100	1120^{+780}_{-380}	$1.16^{+0.41}_{-0.22}$	$-2.16^{+0.51}_{-0.25}$	low-ε (I)	Y / Y	(1,3)
070724A	0.457	0.27	n/a	∼68	$0.003^{+0.001}_{-0.001}$	$-2.51^{+0.24}_{-0.24}$	low-ε (I)	Y / N	(3)
071020	2.142	1.34	n/a	323^{+51}_{-51}	$9.5^{+4.3}_{-4.3}$	$-0.70^{+0.11}_{-0.11}$	high-ε (II)	Y / N	(2)
071227	0.394	1.30	∼100	1000^{+200}_{-200}	$0.22^{+0.08}_{-0.08}$	$-2.56^{+0.14}_{-0.14}$	low-ε (I)	Y / N	(3)
080520	1.545	1.10	n/a	∼30	$0.07^{+0.02}_{-0.02}$	$-0.94^{+0.16}_{-0.16}$	high-ε (II)	Y / N	(6)
080913	6.7	1.04	n/a	121^{+232}_{-39}	$7^{+1.81}_{-1.81}$	$-0.77^{+1.39}_{-0.23}$	high-ε (II)	Y / Y	(4)
090423	8.1	1.13	n/a	54^{+22}_{-22}	10^{+3}_{-3}	$-0.11^{+0.30}_{-0.30}$	high-ε (II)	Y / Y	(7,8)
090426	2.609	0.33	n/a	45^{+57}_{-43}	$0.42^{+0.59}_{-0.04}$	$-0.72^{+0.92}_{-0.69}$	high-ε (II)	Y / Y	(9)
090510	0.903	0.26	n/a	4414^{+420}_{-420}	$3.8^{+2.5}_{-2.5}$	$-2.63^{+0.07}_{-0.07}$	low-ε (I)	Y / N	(10)
100206	0.41	0.12	n/a	439^{+73}_{-60}	$6.15^{+0.39}_{0.39} \times 10^{-2}$	$-2.61^{+0.07}_{-0.07}$	low-ε (I)	Y / N	(11)

REFERENCES. — (1) Butler et al. (2007); (2) Amati et al. (2008); (3) Zhang et al. (2009); (4) Piranomonte et al. (2006); (5) Thoene et al. (2007); (6) Sakamoto et al. (2008); (7) Tanvir et al. (2009); (8) Salvaterra et al. (2009); (9) Levesque et al. (2009); (10) Abdo et al. (2009); (11)Cenko et al. (2010)

* GRB 050724 and GRB 060614 have $T_{90,z}$ slightly longer than 2 s. They are included due to the close analogy with other GRBs in the sample.

Soderberg, A. M., et al. 2004, Nature, 430, 648
Soderberg, A. M. et al. 2008, Nature, 453, 469
Stanek, K.Z., Matheson, T., Garnavich, P.M., et al. 2003, ApJ, 591, L17
Tanvir, N. R., Chapman, R., Levan, A. J., & Priddey, R. S. 2005, Nature, 438, 991
Tanvir, N. R., et al. 2009, Nature, 461, 1254
Thoene, C. C., et al. 2007, GCN, 6379, 1
Villasenor, J.S., Lamb, D.Q., Ricker, G.R., et al. 2005, Nature, 437, 855
Virgili, F. J., Zhang, B., O'Brien, P., & Troja, E. 2009, arXiv:0909.1850
Woosley, S. E. 1993, ApJ, 405, 273
Woosley, S. E., & Bloom, J. S. 2006, ARA&A, 44, 507
Xin, L., et al. 2010, MNRAS,tmp. 1404 (arXiv:1002.0889)
Zhang, B. 2006, Nature, 444, 1010
Zhang, B., Zhang, B.-B., Liang, E.-W., et al. 2007, ApJ, 655, L25
Zhang, B., Zhang, B.-B., Virgili, F.J., et al. 2009, ApJ, 703, 1696

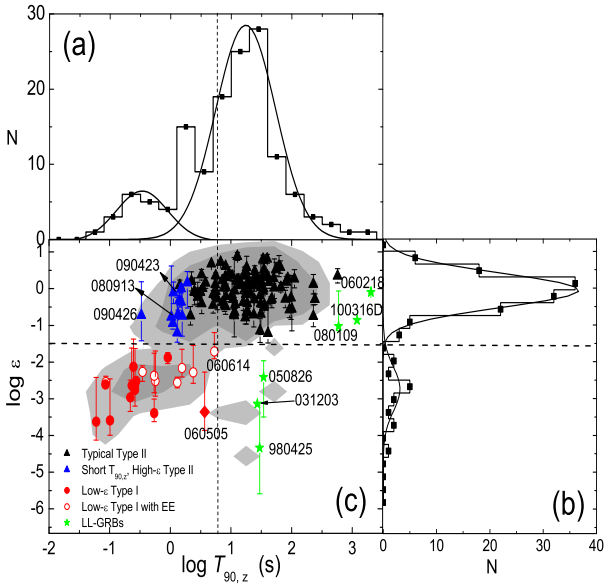

FIG. 1.— The 1-D and 2-D distributions for the bursts in our sample in the $\log T_{90,z}$ *vs* $\log\varepsilon$ plane along with the bimodal fits (*solid lines, in panel a, b*) as well as the 2-D distribution for the GRBs in our sample in the $\log\varepsilon - \log T_{90,z}$ and $\log\varepsilon - \log(1+z)$ plane (*panel c*). The *triangles* denote the Type II GRB candidates as discussed in literature. Among them the traditional long GRBs are denoted as *black* and the GRBs with $T_{90,z} < 2$ s are denoted as *blue*. The *red solid (open) circles* represent the Type I GRBs with (without) extended emission as discussed in the literature. The *diamond* denotes the special burst GRB 060505. Nearby LL-GRBs are denoted as green *stars*. The possibility contours for GRB clustering are marked, with $p\ (\log\varepsilon, \log T_{90,z}) > 0.1$ (*dark grey*) and $p\ (\log\varepsilon, \log T_{90,z}) > 0.003$ (*light grey*), respectively. The dashed vertical and horizontal lines are the divisions of $\varepsilon = 0.03$ and $T_{90,z} = 5$ seconds, respectively.

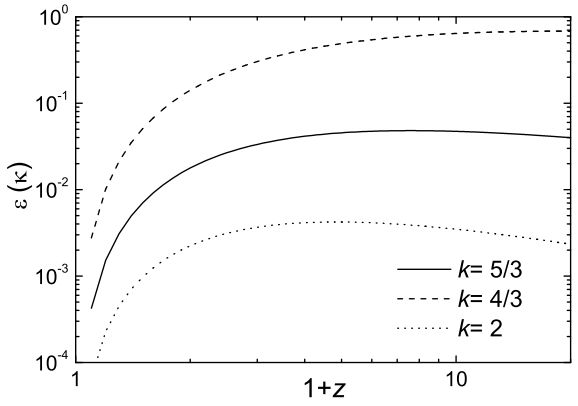

FIG. 2.— Dependence of $\varepsilon(\kappa)$ on $(1+z)$ for $\kappa = 4/3,\ 5/3,\ 2.0$ for a given burst with the same measured fluence and E_p.

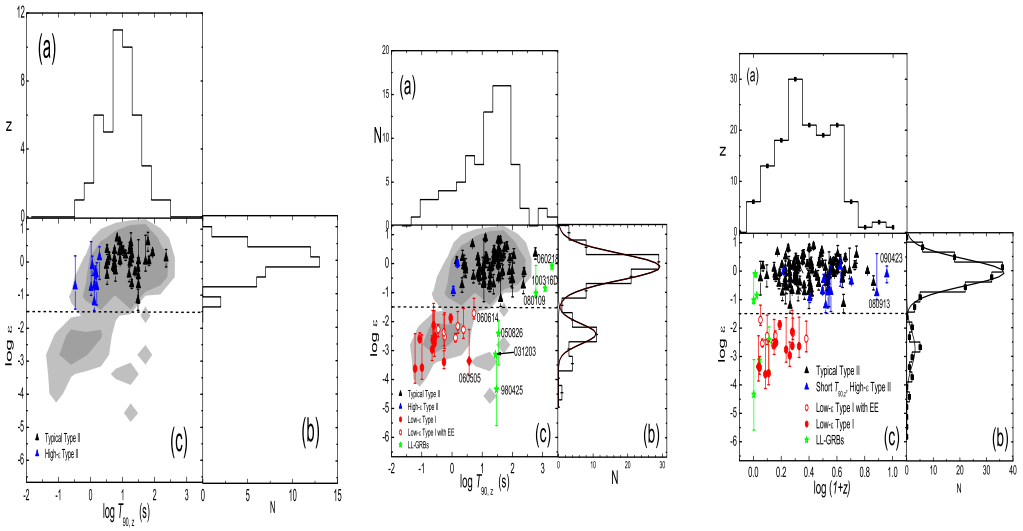

FIG. 3.— The 1-D (*panels a and b*) and 2-D (*panel c*) distributions for the bursts in our sample in the $\log T_{90,z} - \log \varepsilon$ plane for GRBs for $z > 2$ (*left group of panels*) and $z < 2$ (*middle group of panels*). The GRB distributions in the $\log(1+z) - \log \varepsilon$ plane are also shown in the *right group of panels*. The symbol style is the same as Figure 1. The contours are the same as that in Figure 1 for all GRBs in our sample.

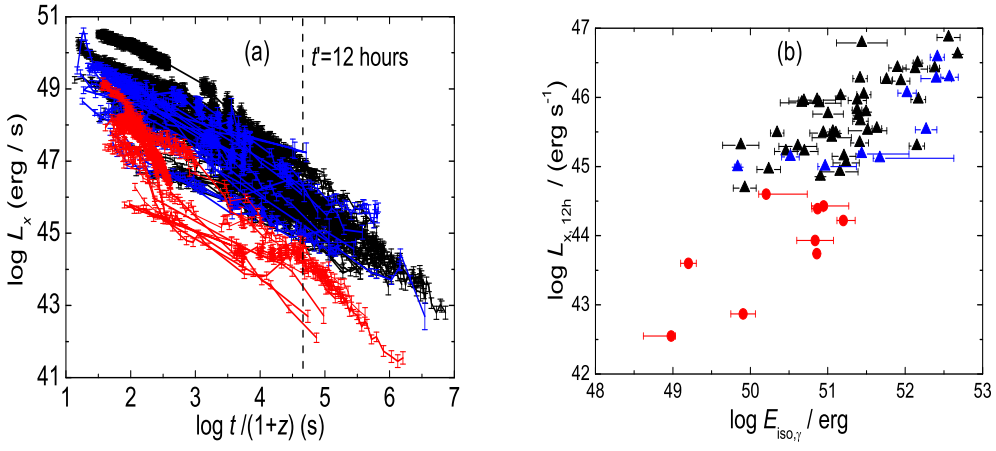

FIG. 4.— Comparisons of (a) the XRT lightcurves and (b) the $L_{X,12h} - E_{\rm iso}$ distribution among the low-ε GRBs with $T_{90,z} < 5$ s (*red*), high-ε GRBs with $T_{90,z} < 2$ s (*blue*), and 44 long-duration high-ε GRBs from the Liang et al. (2009) sample (*black*). Here $L_{X,12h}$ is the X-ray luminosity in the XRT band at the rest-frame 12 hours post the GRB trigger.